ADVANCED ENGINEERING MATERIALS

DOI: 10.1002/adem.201400414

Self-Assembled Recyclable Hierarchical Bucky Aerogels**

By *Mehmet Karakaya, Deepika Saini, Ramakrishna Podila,* Malcolm J. Skove, Apparao M. Rao,* Ramathasan Thevamaran* and *Chiara Daraio*

We describe a simple method for the scalable synthesis of three-dimensional, elastic, and recyclable multi-wall carbon nanotube (MWCNT) based light weight (density <1 g cm^{-3}) bucky-aerogels (BAGs) that are capable of efficiently absorbing non-polar solvents and separating oil-in-water emulsions. Our facile synthesis involves the self-assembly of MWCNTs and carbon fibers into a multi-layered, highly porous, and hierarchical structure that can be easily flexed, compressed, or burnt without any noticeable changes in its structure and absorption capacity. The BAG surface absorbs non-polar solvents efficiently up to ≈20 times its own weight due to its superhydrophobic nature arising from the presence of MWCNTs. Furthermore, BAGs exhibit excellent resilience to impact by recovering more than 70% of the deformation. The energy dissipated by BAGs at 80% compressive strain is in the order of 500 kJ m^{-3}, which is nearly 50 times more than the energy dissipated by commercial foams with similar densities.

1. Introduction

Aerogels are synthetic, ultralight, and highly porous materials known for their low thermal conductivity, low bulk density, and high surface area. These unique properties have led to the use of aerogels in multifunctional applications,[1–3] which include artificial muscles,[1] solar cells,[2] radiation detection,[4] supercapacitor electrodes,[5] and catalysis.[6] Traditionally, aerogels are oxide-based (e.g., SiO_2[7] and SnO_2[8]), however in the recent past, scientists have developed non-traditional hierarchically nanostructured aerogels, viz., multi-walled carbon nanotubes (MWCNTs) films,[9] nanosponges,[10–12] nanofoams,[13] nanowire membranes,[14] and organic and inorganic composites.[15] To date, these hierarchically nanostructured aerogels are either synthesized via chemical vapor deposition (CVD),[10] sol–gel or critical point drying (CPD)[12] techniques, which are not only tedious but lack easy scalability, and use expensive equipment or toxic precursors.[10]

In this article, we demonstrate the fabrication of 3D hierarchical all-carbon aerogel, which we refer to as bucky-aerogel (BAG). We synthesize large BAG samples with tunable porosity and characterize their microstructure, hydrophobicity, and oleophilicity, and mechanical properties. We show that BAG is highly oleophilic across a moderate range of surface tensions (20–40 mN m^{-1}) and displays a strong affinity toward a variety of organic and inorganic solvents. Our top-down synthesis allows for the porosity of BAG to be tuned to facilitate selective absorption of solvents up to 20 times its weight, which is comparable to the performance observed in other nanowire-based sponges and is at least 5–10 times better compared to absorptive properties of activated carbon aerogels.[14] Notably, BAG has the unique ability to absorb oil from oil-in-water (o/w) emulsions, which continues to be a formidable challenge in oil-spill cleanup efforts critically endangering our environment. The absorbed oils/solvents may be efficiently recovered by simply squeezing the BAG, or disposed via burning the BAG under ambient conditions. Lastly, the exceptional MWCNTs properties render BAG highly stable and resistant to harsh

[*] *A. M. Rao, M. Karakaya, D. Saini, R. Podila, M. J. Skove*
Department of Physics and Astronomy, Clemson Nanomaterial Center, Clemson University, Clemson SC 29634, USA
E-mail: arao@g.clemson.edu; rpodila@g.clemson.edu
A. M. Rao
COMSET, Clemson University, Clemson, SC 29634, USA
R. Thevamaran, C. Daraio
Division of Engineering and Applied Sciences, California Institute of Technology, Pasadena CA 91125, USA
Swiss Federal Institute of Technology Zurich (ETH Zurich), Zurich 8092, Switzerland

[**] *A.M.R. acknowledges the support from US National Science Foundation grant CMMI-1246800 award for scalable nanomanufacturing. R. P. and A. M. R. thank Clemson University TIGER grant for supporting this work. C.D. and R.T. acknowledge support from the Institute for Collaborative Biotechnologies under contract W911NF-09-D-0001 with the Army Research Office (Supporting Information is available online from Wiley InterScience or from the author).*

FULL PAPER

chemical exposure (including strong acids), high pressure, and high temperature environments.

2. Results and Discussion

As evident from the scanning electron microscope (SEM) images of a BAG cross-section (Figure 1), vacuum filtration of CFs containing MWCNT dispersions results in a self-assembly of stacked layers of randomly entangled MWCNTs (similar to a MWCNT buckypaper) supported by interpenetrating CFs. The standard N_2 adsorption isotherms (at 77 K) revealed an average mesoporous (2–50 nm, ≈5–7%) and macroporous (1–10 μm, ≈93–95%) size distribution (see Supplementary Information), which stem from the intra- and inter-layer distribution of MWCNT layers (Figure 1). As discussed later, such pore distribution allows an easier access to the BAG interior resulting in a higher absorption capacity.

The wetting angle of ≈160° by a water droplet in Figure 2a implies that the BAGs exhibit superhydrophobicity (contact angle >150°). An obverse response (oleophilicity) was seen for an oil drop, which wets the BAG with a contact angle of ≈35° (Figure 2b) before getting fully absorbed by the BAG. As a result, BAG is an ideal material for separating oil from water due to its highly selective absorption capacity for oil over water.

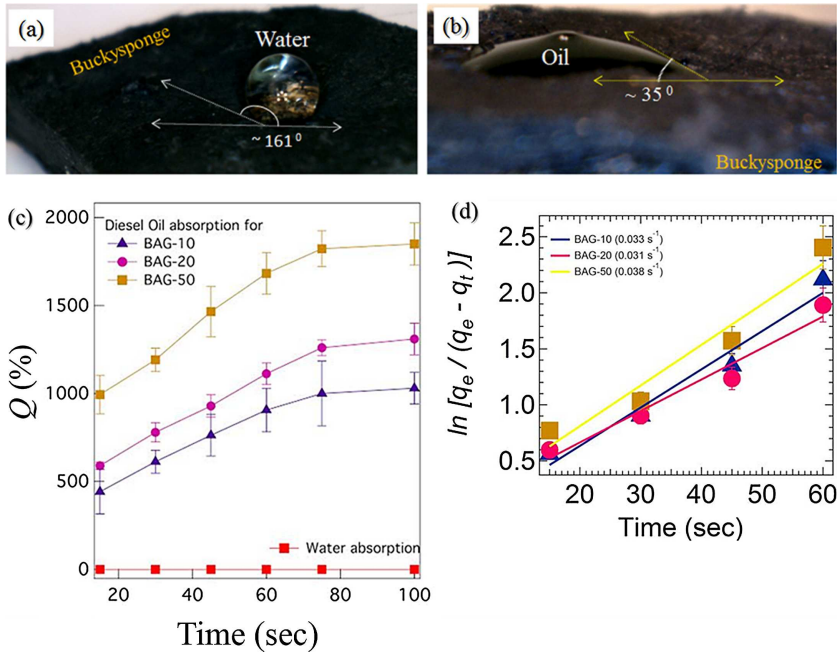

Fig. 2. Panels (a) and (b) depicts a qualitative comparison of the hydrophobic and oleophilic properties of the BAG, respectively. A water droplet exhibits an apparent contact angle of ≈160° and remains on the surface of the BAG while an oil droplet (Fischer vacuum pump oil) gets fully absorbed by the BAG after wetting the BAG with an apparent contact angle of ≈35°. Note that the cosine of apparent contact angle (on a rough surface) is related to the cosine of Young contact angle (on a flat surface) through the roughness ratio. (c) Dependence of the quality factor Q on time and the macroporosity of the BAG. Evidently, the BAG comprised of the highest amount of CFs exhibits the highest Q, or absorbs the maximum oil. (d) The absorption process follows a pseudo-first order rate kinematics. The solid lines show the least square fits to the experimental data and of the corresponding rate constants (k_{p1}) for each sample are indicated within parentheses.

To characterize BAG's absorption efficiency and gauge the influence of its meso- and macro-porosity, we undertook a study in which 10–50 wt% diesel oil (density ≈0.85 g cm^{-3}) was separated from a mixture of oil and water (Figure 2c). Following the immersion of a BAG in the oil–water mixture for a time t, the BAG was weighed after wiping its surface off the unabsorbed oil with a clean razor blade. Based on the amount of absorbed oil, a quality factor Q = (weight after absorption − weight of as-synthesized BAG)/weight of as-synthesized BAG) × 100 for each of the three BAGs was elicited (Figure 2c). The Q for each of the BAGs was found to increase linearly with time, indicating a constant rate of absorption, before attaining a saturation absorption at $t \approx 1$ min. Interestingly, a maximum Q of 1800% was recorded for BAG-50 implying that the amount of oil it absorbed was 18 times its own weight. Such absorptive properties of BAGs are at least 5–10 times better than the traditional activated carbon aerogels.[14] The enhanced Q for BAG-50 compared to those for BAG-10 and BAG-20 is attributed to the increased number of macropores accessible to oil in BAG-50.

The increased macroporosity, as seen in Supplementary Table S1, is due to an increased

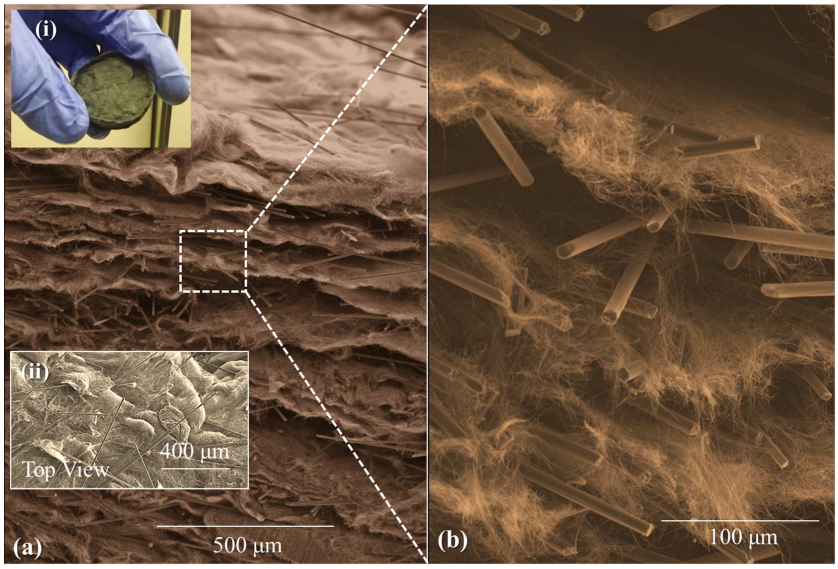

Fig. 1. Scanning electron microscope (SEM) images of as-prepared bucky aerogels (BAGs). (a) The cross-sectional view clearly shows the layered composition of the carbon nanotubes (CNTs) and carbon fibers (CFs). The inset (i) depicts the as-prepared BAG disk, which is robust and easy to handle. The inset (ii) is the SEM image of the BAG top surface, which together with the image in (a) suggests that the BAG is predominatly an entangled microstructure containing sheets of CNTs with inter penetrating CFs. (b) Magnified image of the marked area in panel (a).

ADVANCED ENGINEERING MATERIALS 2014,
DOI: 10.1002/adem.201400414

amount of CFs in the BAG, which in turn increases the interlayer spacing in the BAG (cf. Figure 1). The increased interlayer spacing facilitates transport of a larger amount of oil through the macroporous channels. The absorption is conjectured to be a simple physical process at the macropores corroborated by the exclusively physisorption capacities, which follow the pseudo-first order kinetics[16] (Figure 2d) as described in Equation 1

$$1n\left(\frac{q_e}{q_e - q_t}\right) = k_{p1}t \quad (1)$$

where q_e is the maximum saturated Q, q_t is the Q value at any given time t, and k_{p1} is the pseudo 1st order rate constant. BAG-50 samples exhibited a slightly higher rate constant (Figure 2d) compared to BAG-10 and BAG-20 suggesting that the absorption process is indeed driven through the macroporous channels. Interestingly, the physical absorption and mass transfer play a major role with no evidence for chemisorption in the kinetics, which affirms our hypothesis, and makes BAGs attractive for a wide range of applications due to its tunable macroporosity.

Besides diesel oil, we also investigated BAG-50's capacity to absorb other organic solvents (dimethyl formamide (DMF), ethanol), saturated fats (vegetable oil), and other oils (motor oil). As indicated in Figure 3a, all solvents could be readily separated from their corresponding aqueous mixtures (10–50 wt% in water). DMF was the most absorbed liquid ($Q \approx$ 2000%) while all other liquids exhibited a $Q > 120$ 0%, which is comparable to existing nanowire materials.[17]

In order to retrieve the adsorbed oil, the oil saturated BAG could be either mechanically squeezed, as discussed in the later section, or ignited to burn off the oil and reused, thus facilitating energy harvesting as heat (see video 1 in Supplementary Information). To test this hypothesis, we allowed BAG-50 to absorb regular pump oil for 15 s and then subsequently burnt it to release 736 kJ of heat energy. We measured the released energy by heating de-ionized water and measuring the change in the temperature (ΔT) of 100 ml water in a glass beaker using a thermocouple (Omega J thermocouple, part number CHAL-32). Considering heat capacity of water (c_w) to be 4186 J kg^{-1} °C, we obtained the heat energy as $E = mc_w\Delta T$ to be 736 kJ, where m is the mass of water. The oil burns at about 300 °C, which is not high enough to damage the BAG's carbon constituents. Hence, even after prolonged and repeated burning, the layered morphology, flexural, and absorption properties of the BAGs remained intact (Figure 3b) with no measurable mass loss.

One of the bigger challenges currently faced by the petroleum industry is to separate oil from its emulsion phase. Hence, we tested the BAG's performance in separating oil and water from two oil-in-water (o/w) emulsions with 50 and 33% (by wt) oil. The emulsion was prepared by tip sonicating oil (density ≈820 mg ml^{-1}) with water (density 991 mg ml^{-1}). The density of the emulsion was measured to be 908 mg ml^{-1} (50% o/w emulsion) and 934 mg ml^{-1} (33% o/w emulsion). A BAG-50 was then immersed in the emulsion in a petri dish. After 5 min, the oil saturated BAG was removed, and the density of the remaining emulsion increased to 976.3 mg ml^{-1} (50% o/w emulsion) and 951.26 mg ml^{-1} (33% o/w emulsion). This dramatic increase in the final density arose from 90% removal of oil from the emulsion confirming that BAG is an effective emulsion separator.

Another unique attribute of the BAG is its ability to deform elastically under an applied external force, and revert to its original shape upon removal of the external force. This elasticity of the BAG is essential for efficient recovery of absorbed liquids (also see Videos 2 and 3 in Supplementary Information). To characterize its mechanical performance, we performed strain-controlled quasistatic compression tests at 0.01 s^{-1} strain-rate. The characteristic loading–unloading stress–strain responses of BAG-10, BAG-20, and BAG-50 samples up to 80% compression are shown in Figure 4a. When a BAG sample is compressed, it exhibits a foam-like response, i.e., the stress increases nonlinearly with strain up to the peak stress, and then follows a rapid unloading along a different stress–strain path, forming a hysteresis loop. The presence of this hysteresis, similar to other foam materials,[18] is responsible for the dissipation of mechanical energy. On an average, BAGs dissipate ≈500 kJ m^{-3} energy in the initial compression cycle, which is more than 50 times higher than the energy dissipated by commercial polymeric foams with comparable bulk densities.[18]

BAG-20 (with 20% CFs) exhibits a stiffer response compared to BAG-10 (with 10% CFs), as expected, due to the increased presence of CFs in the former. However, BAG-50 (with 50% CFs) exhibits a more compliant response, which is a result of its relatively high porosity. To evaluate the

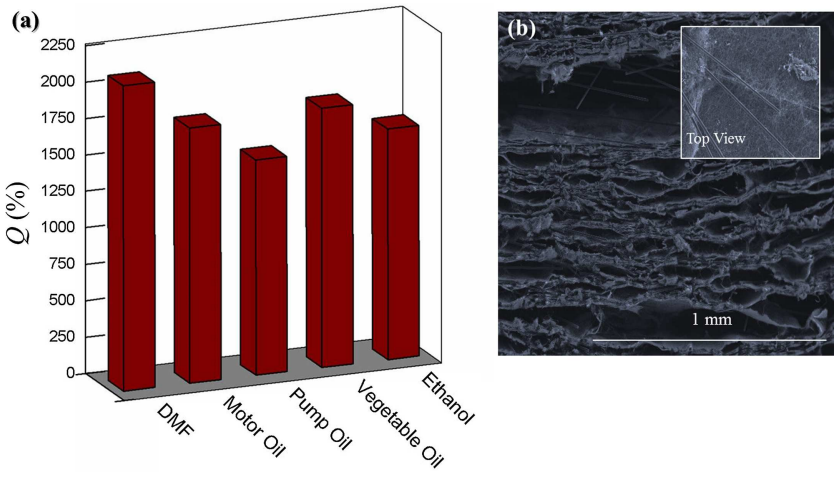

Fig. 3. (a) The Q plotted for a variety of organic liquids. (b) A SEM image of the cross-section of a burnt BAG-50 with its layered architecture (cf. Figure 1) left intact with no noticeable deterioration in its physical and absorptive properties.

DOI: 10.1002/adem.201400414

FULL PAPER

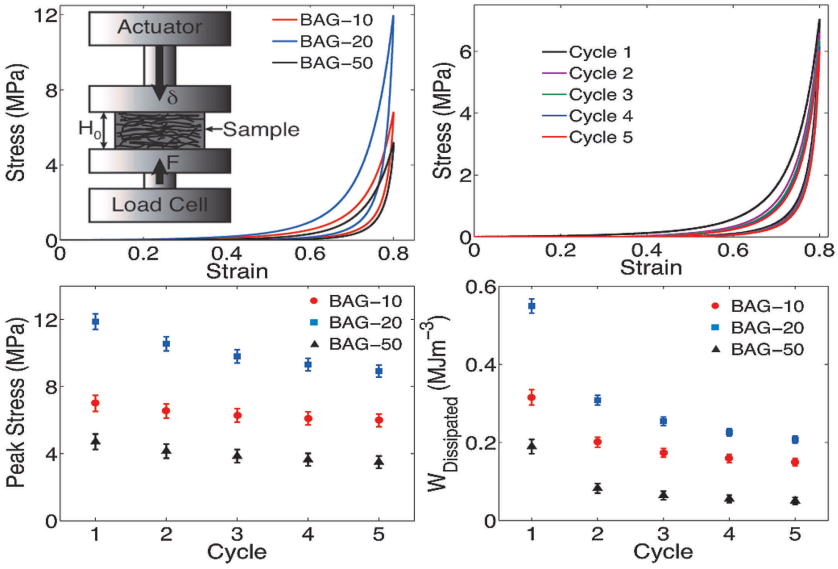

Fig. 4. Mechanical response. (a) Characteristic stress–strain responses of BAG-10, BAG-20, BAG-50 samples; the inset shows a schematic of the test setup. (b) Cyclic compression response of a BAG-10 sample. (c) Variation of peak stress values reached in consecutive cycles. (d) Variation of the energy dissipation with consecutive cycles.

robustness of the BAG materials, we performed quasistatic cyclic compression tests. Figure 4b shows the characteristic response of a BAG-10 sample for five consecutive cycles. All samples exhibit preconditioning effects – the first cycles follow a different loading path than the consecutive cycles. This preconditioning effect, common in MWCNT materials,[19] is more pronounced in the first three cycles, beyond which the response of the samples stabilizes to a repeatable loading–unloading path. The preconditioning is also evident in the measured peak stress and energy dissipation as a function of the number of loading cycles (Figure 4c and d). For example, for the BAG-10, the peak stress decreases by ≈15% in the first three cycles, and remains nearly constant in the following cycles. The energy dissipation decreases ≈45% in the first three cycles and remains nearly constant in the consecutive cycles. Importantly, all samples show an average recovery of ≈50% in compression even after repeated cycles at 80% strain. This ability to recover large deformation is important in oil absorption applications. Since the oils/solvents are physisorbed by the BAG, it is possible to retrieve most of the absorbed oil/solvent by simply squeezing the saturated BAG without compromising the BAG structure. In other words, after squeezing out the physisorbed oil, the BAG reverts to its original shape and can be reused (see Supplementary Information).

3. Conclusions

The self-assembly of an inter-connected network of MWCNTs and carbon fibers (CF) can be used to synthesize hierarchical BAG structures with controlled porosity. BAGs exhibit excellent oil/solvent absorption properties (as much as 20 times their weight) for a variety of solvents (surface tensions: 20–40 mN m^{-1}). More importantly, BAGs can efficiently separate oil not only from slicks but also from oil-in-water emulsions with ≈90% efficiency. More importantly, BAGs exhibit a highly nonlinear foam-like stress–strain response with hysteretic dissipation and high-strain recovery.

4. Experimental Section

For preparing a BAG, ≈50 mg MWCNTs (Sai Global Technologies, Inc., San Antonio, TX, dia: 30–50 nm) were added to 1 wt% sodium dodecyl sulfate (SDS: 100 ml) aqueous solution. About 10, 20, and 50 wt% CF (avg dia 8 μm) were added to this mixture and tip sonicated (Branson Sonifier 200 Watt) for 10–15 min (at 40% power) to prepare a homogenous dispersion in the SDS solution. Subsequent to vacuum filteration through a nylon filter membrane (Whatman, 0.45 μm), three different BAGs (labeled as BAG-10, BAG-20, and BAG-50) were obtained. Following a heat treatment in air at 70 °C for 30 min, each BAG was peeled off the filter paper as a free standing disc (inset (i) of Figure 1a). When the loading of CF exceeded 50 wt%, the above procedure did not yield a BAG, presumably due to the insufficent amount of MWCNTs to form a robust network in which the CFs could be held. Scanning electron microscopy characterization was performed using Hitachi S-3400N. The contact angle was determined from the optical images obtained using a tabletop Celestron 100× microscope and imageJ software. For characterizing the oil absoprtion ability, a known mass of BAG sample was allowed to adsorb oil and then weighed later to measure the absorbed oil. The mechanical performance of the BAG structures was tested using commercial testing system (Instron ElectroPulse E3000).

Received: September 10, 2014
Final Version: October 16, 2014

[1] A. E. Aliev, J. Oh, M. E. Kozlov, A. A. Kuznetsov, S. Fang, A. F. Fonseca, R. Ovalle, M. D. Lima, M. H. Haque, Y. N. Gartstein, M. Zhang, A. A. Zakhidov, R. H. Baughman, *Science* **2009**, *323*, 1575.
[2] T. W. Hamann, A. B. F. Martinson, J. W. Elam, M. J. Pellin, J. T. Hupp, *Adv. Mater.* **2008**, *20*, 1560.
[3] J. T. Korhonen, P. Hiekkataipale, J. Malm, M. Karppinen, O. Ikkala, R. H. A. Ras, *ACS Nano* **2011**, *5*, 1967.
[4] L. Cremaldi, D. A. Sanders, P. Sonnek, D. J. Summers, J. Reidy, *Nuclear Sci., IEEE Trans.* **2009**, *56*, 1475.
[5] G. R. Li, Z. P. Feng, Y. N. Ou, D. C. Wu, R. W. Fu, Y. X. Tong, *Langmuir* **2010**, *26*, 2209.

DOI: 10.1002/adem.201400414

ADVANCED ENGINEERING MATERIALS

[6] C. Moreno-Castilla, F. J. Maldonado-Hodar, *Carbon* **2005**, *43*, 455.
[7] M. Moner-Girona, A. Roig, E. Molins, J. Llibre, *J. Sol-Gel Sci. Technol.* **2003**, *26*, 645.
[8] T. F. Baumann, S. O. Kucheyev, A. E. Gash, J. H. Satcher, *Adv. Mater.* **2005**, *17*, 1546.
[9] J. T. Di, D. M. Hu, H. Y. Chen, Z. Z. Yong, M. H. Chen, Z. H. Feng, Y. T. Zhu, Q. W. Li, *ACS Nano* **2012**, *6*, 5457.
[10] X. C. Gui, Z. P. Zeng, Y. Zhu, H. B. Li, Z. Q. Lin, Q. M. Gan, R. Xiang, A. Y. Cao, Z. K. Tang, *Adv. Mater.* **2014**, *26*, 1248.
[11] H. B. Li, X. C. Gui, L. H. Zhang, S. S. Wang, C. Y. Ji, J. Q. Wei, K. L. Wang, H. W. Zhu, D. H. Wu, A. Y. Cao, *Chem. Commun.* **2010**, *46*, 7966.
[12] S. M. Jung, H. Y. Jung, M. S. Dresselhaus, Y. J. Jung, J. Kong, *Sci. Rep.-UK*, **2013**, *3*, 2, Article No. 1423.
[13] P. Calcagnile, D. Fragouli, I. S. Bayer, G. C. Anyfantis, L. Martiradonna, P. D. Cozzoli, R. Cingolani, A. Athanassiou, *ACS Nano* **2012**, *6*, 5413.
[14] J. K. Yuan, X. G. Liu, O. Akbulut, J. Q. Hu, S. L. Suib, J. Kong, F. Stellacci, *Nat. Nanotechnol.* **2008**, *3*, 332.
[15] P. Thanikaivelan, N. T. Narayanan, B. K. Pradhan, P. M. Ajayan, *Sci. Rep.-UK*, **2012**, *2*, 2, Article No. 230.
[16] Y. H. Han, X. Quan, S. Chen, H. M. Zhao, C. Y. Cui, Y. Z. Zhao, *Sep. Purif. Technol.* **2006**, *50*, 365.
[17] L. J. Gibson, M. F. Ashby, *Cellular Solids*, Cambridge University Press, Cambridge, UK **1997**.
[18] A. Misra, J. R. Raney, L. De Nardo, A. E. Craig, C. Daraio, *ACS Nano* **2011**, *5*, 7713.
[19] J. Suhr, P. Victor, L. C. S. Sreekala, X. Zhang, O. Nalamasu, P. M. Ajayan, *Nat. Nanotechnol.* **2007**, *2*, 417.